JOURNAL OF APPLIED ELECTROCHEMISTRY 23 (1993) 559–566

Cathodic behaviour of IrO_2 electrodes in alkaline solution
Part I: Electrochemical surface characterization*

H. CHEN‡, S. TRASATTI§

Department of Physical Chemistry and Electrochemistry, University of Milan, Via Venezian 21, 20133 Milan, Italy

Received 15 June 1992; accepted 30 July 1992

IrO_2 electrodes prepared by thermal decomposition of $IrCl_3$ on a titanium support at temperatures of calcination between 300 and 500° C have been characterized by cyclic voltammetry and potential steps. 'Standard' voltammetric curves have been recorded between −0.65 and 0.35 V vs SCE (prior to H_2 and O_2 evolution) as a 'fingerprint' of the surface state, and the associated charge, q^*, has been used to monitor the morphology of the active layer. The effect of hydrogen evolution has been investigated by progressively decreasing the negative potential limit, and by increasingly holding the electrode under hydrogen evolution at a constant potential. Phenomena of proton penetration beneath the 'outer' surface into an 'inner' surface have been quantified by potential step experiments. The effect of storing the electrodes in water rather than in the open air has also been investigated. The thermal oxides lose their typical features at calcination temperature < 350° C. Cathodic load does not appear to cause macroscopic modifications of the surface state.

1. Introduction

Thermally prepared electrodes consisting of transition metal oxides were originally proposed for *anodic* processes such as chlorine and oxygen evolution: this is obvious from the acronym DSA® (dimensionally stable anodes) by which they are universally known [1–3]. Recent patents have claimed their use also as *cathodes* for hydrogen evolution [4–7].

Fundamental studies on the cathodic behaviour of DSA®-type materials are very scanty [8–10], with most of them having originated from this laboratory [11]. In particular, hydrogen evolution has been investigated with IrO_2 and RuO_2 electrodes in acidic solution [12,13]. Only a few preliminary data are presently available for hydrogen evolution in alkaline solution [14], a more common environment for technological applications. We have therefore performed a systematic study of the cathodic behaviour of thermal IrO_2 electrodes in 1 M NaOH solutions. The surface characterization by electrochemical techniques is reported in this paper (Part I), while the kinetics of hydrogen evolution will be described in Part II.

2. Experimental details

The electrodes used in this work were not freshly prepared for this specific study but they had already been subjected to extensive anodic and cathodic treatments. One of the goals of this work has been to investigate the behaviour of 'aged' electrodes. The details of the preparation can be found in previous papers [12,13,15]. Briefly, IrO_2 was prepared by thermal decomposition of about 0.03 M *aqueous* solutions of $IrCl_3 \cdot nH_2O$ (Ventron) (note that the solvent affects the properties [15]) on both sides of titanium platelets of 1 cm^2 apparent surface area. The special Teflon holder has been described elsewhere [16]. Two samples were prepared at each of the following temperatures: 300, 330, 360, 400, 450, 500° C. The apparent oxide loading was about 1.2 mg cm^{-2}, corresponding to a nominal thickness of about 1 μm. The physico-chemical characteristics of such layers have been described previously [17].

1 M NaOH aqueous solutions, prepared with Fluka chemicals (puriss. p.a.) and Milli-Q water, were used throughout the work with the exception of reaction order determinations for which 1 M constant ionic strength solutions of NaOH + $NaClO_4$ were employed. Solutions were deaerated by bubbling purified nitrogen gas for one hour before each run, and constantly during the run (thus providing some stirring).

The three-compartment cell has been described elsewhere [18]. Electrode potentials were measured against a satd. calomel electrode (SCE) systematically checked against a second electrode (constantly

* This paper is dedicated to Professor Brian E. Conway on the occasion of his 65th birthday, and in recognition of his outstanding contribution to electrochemistry.

‡ Permanent address: Fujian Institute of Research on the Structure of Matter, Chinese Academy of Sciences, Fuzhou, Fujian, People's Republic of China.

§ To whom all correspondence should be addressed.

0021-891X

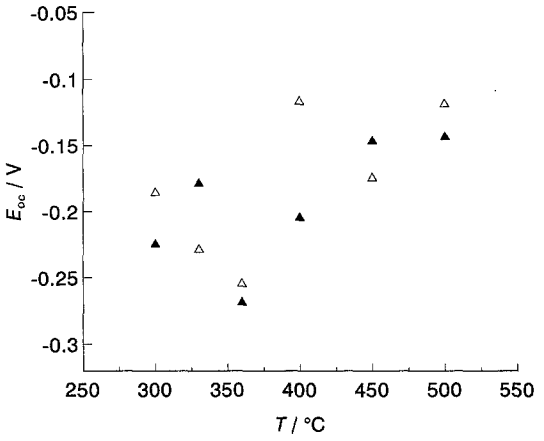

Fig. 1. Open circuit potential of IrO_2 electrodes in 1 M NaOH solution as a function of the calcination temperature. Samples permanently stored in water (▲) and in air (△) are distinguished.

immersed in satd. KCl) before and after each run. The temperature was controlled to ± 0.1° C by means of a water thermostat. Unless otherwise stated, experiments were conducted at 25° C.

The electrochemical surface characterization was carried out by cyclic voltammetry and potential steps using AMEL instrumentation (models 549 potentiostat, 566 function generator, 631 differential electrometer and 862 X–Y recorder). In all cases, current–time curves were integrated graphically.

3. Results and discussion

Electrodes were split into two series. Those in one of the series had been permanently stored in distilled water since the beginning of their use. The other series had been, and continued to be, stored in the laboratory air between experiments. The scope has been to investigate if different conditions of wetting can affect the electrochemical response. This aspect was already explored in a previous paper, but using freshly prepared electrodes [12].

3.1. *Open-circuit potential E_{oc}*

Figure 1 shows the dependence of the open-circuit potential of IrO_2 electrodes on the calcination temperature. While no systematic effect of the conditions of electrode storage can be recognized, a distinct minimum is visible at 350 °C. E_{oc} is more or less constant at lower as well as at higher temperatures, but a more negative value is apparent at $T < 350$ °C.

E_{oc} is determined by surface acid-base as well as redox equilibria. In alkaline solution the surface of IrO_2 is strongly negative since its point of zero charge (p.z.c.) is < 1 [19]. On the SHE-scale the value of E_{oc} for the electrodes prepared at $T > 400$° C ranges from 0.90 to 0.95 V. This value does not differ appreciably from that measured in acid solution [15], which suggests that the surface equilibrium is the same, i.e. formally:

$$IrO_2 + H_2O + e^- \leftrightarrow IrOOH + OH^- \quad (1)$$

The standard potential for the IrO_2/Ir_2O_3 couple is reported to be 0.926 V vs SCE [20].

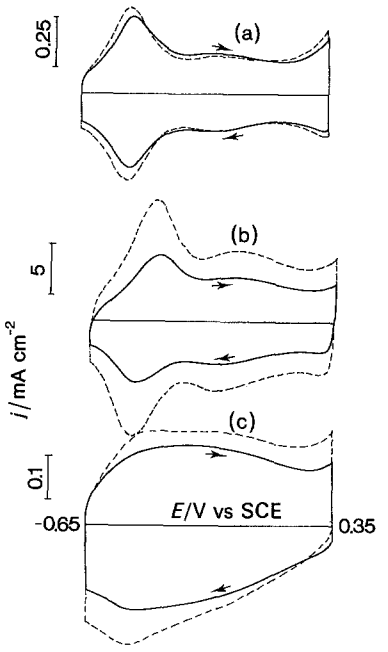

Fig. 2. Voltammetric curves recorded at 20 mV s^{-1} in 1 M NaOH solution of IrO_2 electrodes calcined at different temperatures: (a) 300; (b) 360 and (c) 450° C. (——) Electrodes stored in air. (– – –) Electrodes stored in water.

At $T < 350$° C, the more negative (by about 50 to 100 mV) E_{oc} suggests that the surface oxidation state is probably not the same, the surface being presumably less oxidized. This probably implies that the thermal decomposition process does not go to completion at such low temperatures.

The minimum value at 350° C is unlikely to indicate a further different oxidation state. More probably, it involves a mixed potential with the titanium support. This is possible if the underlying metal comes in contact with the solution. Such a situation can occur if the overlayer is highly porous and, therefore, permeable to the solution [21].

3.2. *Voltammetric curves*

Voltammetric curves, recorded at 20 mV s^{-1} between -0.65 and 0.35 V vs SCE were used as 'fingerprints' of the electrode surface since they constitute an 'electrochemical spectrum' [17]. Figure 2 shows some typical curves for electrodes calcined at different temperatures. No difference can be observed as for the different conditions of electrode storage.

In accord with the features of E_{oc}, the effect of the calcination temperature is remarkable. The electrodes prepared at $T \geqslant 400$° C exhibit a featureless voltammogram typical of DSA®-type oxide electrodes. The electrodes prepared at $T \leqslant 360$° C exhibit pairs of well developed peaks at about -0.45 V vs SCE whose relative height decreases with increasing temperature. It is clear that the chemical state of the surface is different for the two groups of electrodes.

The peak position shifts with temperature for the group of low-T electrodes. More specifically, the anodic–cathodic distance, ΔE, is 10–20 mV at 300° C, 50–70 mV at 330° C, and about 100 mV at 360° C. It

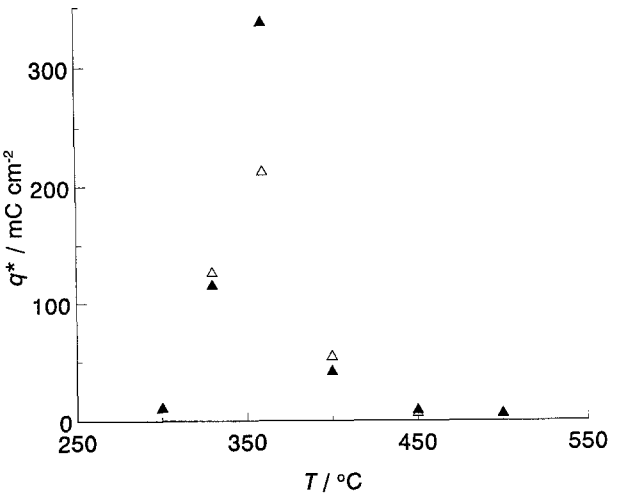

Fig. 3. Voltammetric charge at 20 mV s^{-1} in 1 M NaOH solution vs the temperature of IrO_2 electrode preparation. Samples stored in water (▲) and in air (△) are distinguished.

seems realistic to attribute the observation of a ΔE to the occurrence of an uncompensated ohmic drop. Therefore, the presence of a ΔE can be related to the presence of a non-conducting layer. Since ΔE is minimum at 300° C, the ohmic drop should not be localized in the IrO_2 layer. Rather, it should be localized at the interlayer between the support and the active layer, and is probably due to the presence of insulating TiO_2. At 360° C the presence of TiO_2 and the minimum E_{oc} converge to indicate that the IrO_2 overlayer is very porous so that the underlying metal remains partly uncovered, thus being easily oxidizable.

A hint of a peak is still visible at 400° C and perhaps at 450° C but it disappears completely at 500° C. This may indicate that the group of high-T oxides are fully decomposed so that dry oxygen-bridges are formed. The low-T oxides are probably incompletely decomposed thus acquiring a partly hydrous nature which makes their voltammogram resemble that of anodic IrO_x.

3.3 *Voltammetric charge, q**

Figure 3 shows the dependence of the voltammetric charge, obtained by integration of the curves in Fig. 2, on the calcination temperature. To some extent, the pattern is opposite to that in Fig. 1, with a sharp maximum at 360° C. The voltammetric charge has been shown [17] to be proportional to the number of active sites which can exchange protons with the solution upon potential cycling

$$IrO_x(OH)_y + \delta H_2O + \delta e^- \leftrightarrow IrO_{x-\delta}(OH)_{y+\delta} + \delta OH^- \quad (2)$$

Thus, q^* can be regarded as a relative measure of the active surface area [22].

The temperature of 360° C is probably the 'watershed' between two processes. At $T < 360°$ C thermal decomposition of $IrCl_3$ is still incomplete, therefore the surface charge increases with T because finer particles are formed as more decomposition takes place. At

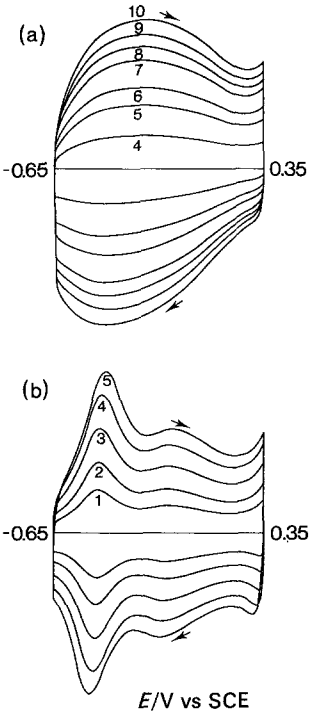

Fig. 4. Voltammetric curves at different potential sweep rates in 1 M NaOH solution of IrO_2 electrodes stored in air. Temperature of preparation: (a) 450° C; (b) 330° C. Sweep rate: (*1*) 2; (*2*) 5; (*3*) 10; (*4*) 20; (*5*) 40; (*6*) 60; (*7*) 80; (*8*) 100; (*9*) 150; (*10*) 200 mV s^{-1}. Current not in scale.

$T > 360°$ C crystal growth and sintering prevail since thermal decomposition is already almost at completion.

Again, no systematic dependence on the conditions of storage are observed in Fig. 3. A somewhat poorly irreproducible behaviour is observed at 360° C, but this is attributed to the cruciality of this temperature at which thermal decomposition and crystal growth proceed at comparable rates.

It is notable that the highest q^* values are observed at 330 and 360° C, the same temperatures where anomalies have been observed in E_{oc} and in the voltammogram. The high values of q^* confirm the high porosity, more at 360 than at 330° C, of these samples.

3.4. *Effect of potential scan rate*

In order to gain insight into the processes occurring at the oxide/solution interface, voltammetric curves were recorded at ten different scan rates between 2 and 200 mV s^{-1}, and the related q^*s were obtained.

Figure 4 shows that the basic features of the voltammogram do not change with scan rate for both low-T and high-T electrodes. As expected, noticeable distortion due to uncompensated ohmic drop is observed with electrodes prepared at 330° C and, more appreciably, at 360 °C.

While the general voltammetric pattern does not vary with scan rate, the voltammetric charge q^* does change dramatically. This is shown in Fig. 5 for three electrodes. For the more porous layers, repeated potential cycling at different speeds appears to induce instability. Actually, for sample 1, Fig. 5 shows that

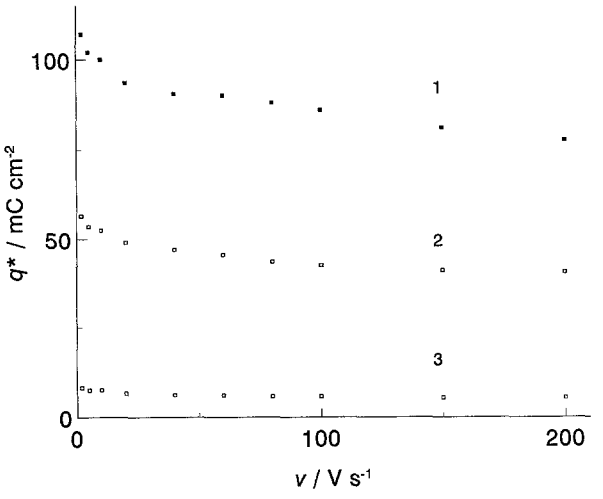

Fig. 5. Dependence of the voltammetric charge of IrO_2 electrodes on the potential sweep rate. Temperature of preparation: (*1*) 330; (*2*) 400; (*3*) 500° C. Storage: (*1*) Water; (*2,3*) Air.

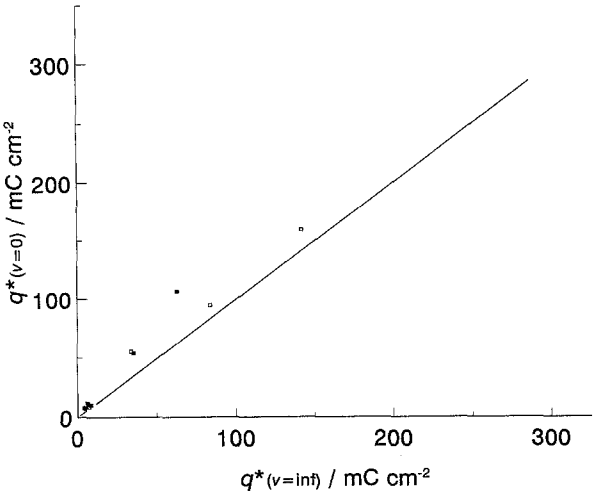

Fig. 7. Voltammetric charge at zero scan rate from Fig. 6a against voltammetric charge at infinite scan rate from Fig. 6b for IrO_2 electrodes stored in water (■) and in air (□). (——) Unit slope.

the decrease of q^* with v is non-monotonic thus suggesting that the morphology of the layer undergoes modifications.

In a previous paper from this laboratory [23], the decrease of q^* with v has been interpreted as evidence of a diffusion-limited step involving proton permeation through cracks, pores, crevices and loose grain boundaries. Therefore, in accord with previous approaches, q^* has been plotted as a function of v in a form related to diffusion processes. Figure 6a shows a typical example of plots of $1/q^*$ against $v^{1/2}$. The remarkably linear dependence can be extrapolated to $v = 0$ to obtain $q^*(v = 0)$, the charge associated with infinitely slow proton exchange. Such a charge can be related to the total active surface available at the oxide/solution interface.

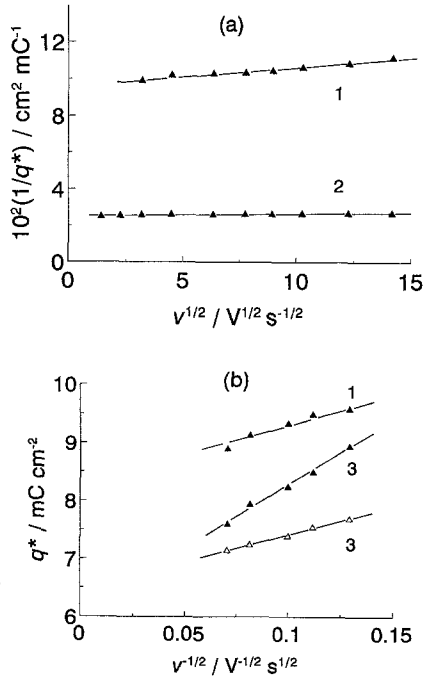

Fig. 6. (a) Reciprocal charge against square root of potential sweep rate and (b) voltammetric charge against reciprocal square root of potential sweep rate for IrO_2 electrodes stored in water (▲) and in air (△). Temperature of calcination: (*1*) 300; (*2*) 400 and (*3*) 450° C.

On the other hand, Fig. 6b shows typical plots of q^* against $1/v^{1/2}$. A linear relationship is also obtained but only from 60 to 200 mV s^{-1}, while at lower scan rate the v scale stretches too much and q^* tends apparently to level off. Extrapolation to $1/v^{1/2} = 0$, i.e. to $v = \infty$, gives the apparent value of $q^*(v = \infty)$, the charge measured as proton diffusion is frozen. Such a charge can be associated with the 'outer' active surface, the 'inner' surface remaining excluded. The relation between the two types of charge is

$$q_t^* = q_i^* + q_o^* \qquad (3)$$

where q_t^* is the charge measured at any finite scan rate. In view of the nature of these quantities, q_o^* is, in principle, expected to be independent of v, the whole dependence being attributed to q_i^*.

The 'inner' and 'outer' surfaces are intimately related. This is shown in Fig. 7 where $q^*(v = 0)$ is plotted against $q^*(v = \infty)$. It is evident that the two quantities are linearly correlated irrespective of the conditions of storage. The linear correlation in Fig. 7 entails that the ratio between the 'outer' and the 'inner' surface is a constant within the experimental accuracy. This is not unreasonable considering that surface area and crystallite size are interrelated, and that the pore volume is also related to the crystallite size. Thus, $q^*(v = 0) - q^*(v = \infty) = q_i^*$ can be regarded as a measure of porosity. For the samples with the higher surface charge, i.e. those prepared at 330 and 360° C, some evidence actually exists in Fig. 7 that q_i^* is higher for the electrodes stored in water.

3.5. *Potential step experiments*

In the above experimental arrangement the proton diffusion layer cannot adequately develop since the diffusion front is perturbed by the potential scan. Moreover, potential scanning does not ensure that real equilibrium conditions can be obtained by

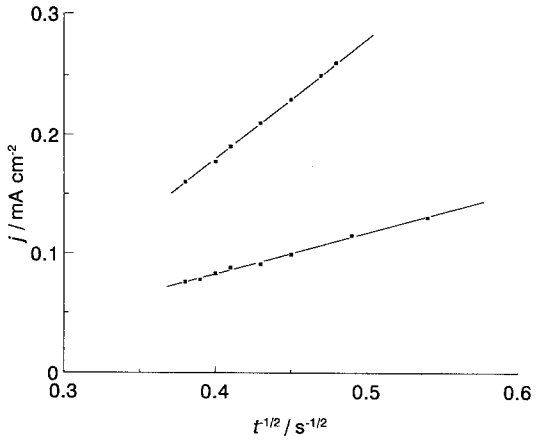

Fig. 8. Current upon potential stepping from 0 to −0.45 V vs SCE against reciprocal square root of time for IrO_2 electrodes prepared at (*1*) 400° C (stored in air) and (*2*) 500° C (stored in water).

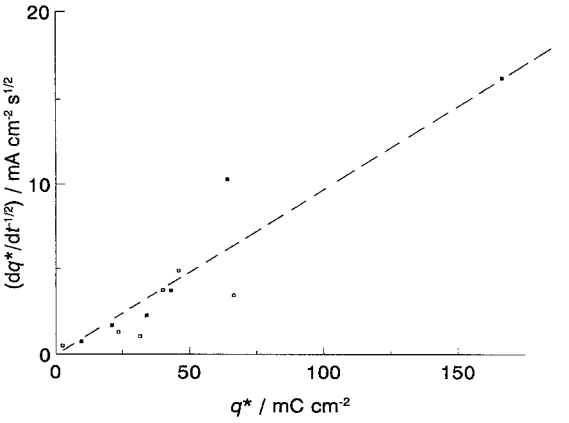

Fig. 10. Slopes of the straight lines in Fig. 8 against the voltammetric charge measured after potential step experiments for IrO_2 electrodes stored in water (■) and in air (□).

extrapolation to $v = 0$. Conversely, proper conditions of diffusion are established with potential steps. Therefore, the potential of the electrode was stepped from 0 to −0.45 V vs SCE and the current recorded.

Figure 8 shows a strictly linear dependence of j on $1/t^{1/2}$, which conforms well to a diffusion-limited process [24]. Integration of the current and extrapolation to $t = \infty$, i.e. $1/t^{1/2} = 0$, gives the total charge which can be accommodated in the active oxide layer. While the absolute value of q^* has no definite meaning, since the graphical integration can only give q^* + const, the slope of the lines $dq^*/dt^{-1/2}$ (or $dj/dt^{-1/2}$) should measure the variation of q_i^* with time, i.e. the rate of the diffusion process. The slope can thus be regarded as a measure of the diffusion front, i.e. of the porosity of the sample.

Figure 9 shows the dependence of the 'electrochemical porosity' on the calcination temperature. Also in this case the electrode behaviour does not show any systematic dependence on the conditions of electrode storage. In fact, a correlation exists between the voltammetric q^* and $dq^*/dt^{-1/2}$ from potential steps, (Fig. 10) although scatter is observed, irrespective of storage conditions.

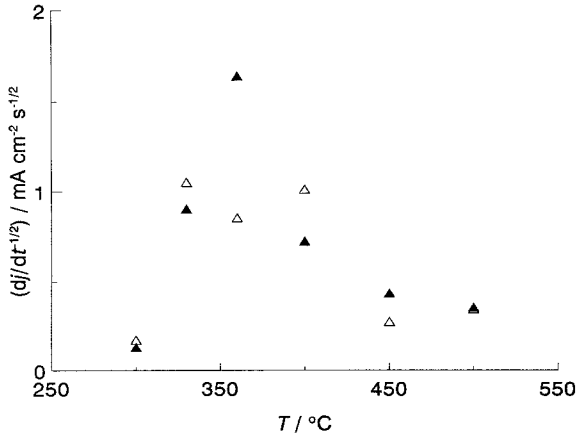

Fig. 9. Slopes of the straight lines in Fig. 8 against the temperature of IrO_2 preparation for electrodes stored in water (▲) and in air (△).

3.6. *Effect of the negative potential limit*

As a preliminary investigation of the stability of the oxide surface toward cathodic load, the samples were subjected to a cyclic potential scan while the negative potential limit was systematically lowered by 0.1 V after each cycle from −0.65 V vs SCE to a potential just prior to hydrogen evolution.

As shown in Figs 11a and 12a, two different patterns are observed depending on the calcination temperature. For the electrodes prepared at $T \leqslant 360°$ C, Fig. 11a, the cathodic potential limit does not change the shape of the curve at $E > -0.65$ V. This indicates that the current flowing at $E < -0.65$ V does not involve proton injection into the active layer. The whole curve strikingly resembles that of an iridium electrode covered with a thick layer of hydrous oxide [25]. Therefore, hydrogen evolution does probably take place on a reduced metallic surface. The well developed

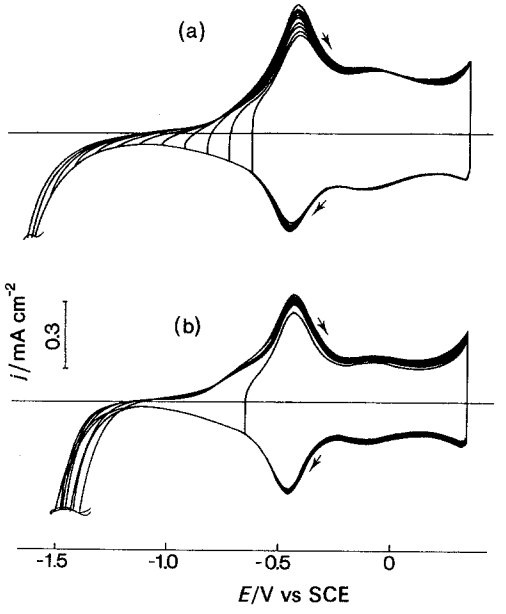

Fig. 11. Effect of (a) the negative potential limit, changed in 0.1 V steps, and (b) the time of hydrogen evolution at −1.65 V vs SCE on the voltammetric curve of IrO_2 electrodes calcined at (a) 330° C, stored in air, and (b) 300° C, stored in water. The time of hydrogen evolution, varied between 10 s and 10 min, is not indicated. The height of the anodic peak increases only slightly with this time.

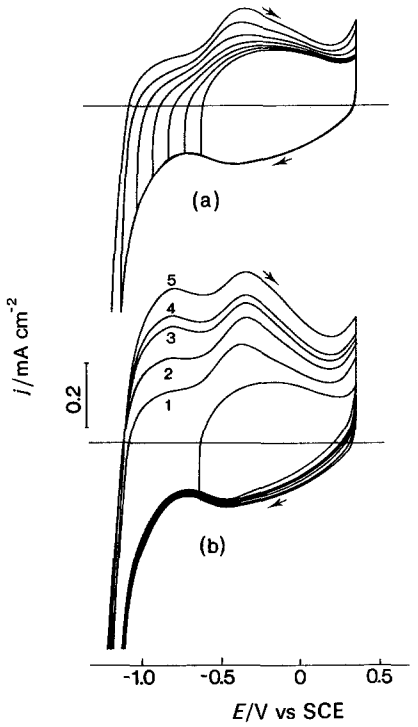

Fig. 12. Effect of (a) the negative potential limit and (b) the time of hydrogen evolution at −1.25 V vs SCE on the voltammetric curve of a IrO_2 electrode calcined at 500° C and stored in air. Time: (*1*) 10 s, (*2*) 30 s, (*3*) 1 min, (*4*) 5 min, and (*5*) 10 min.

peak at −0.45 V vs SCE presumably represents the IrO → Ir transition. Under similar circumstances the charge under the peak is associated with *bulk* proton penetration, and this explains why the charge and the apparent porosity of the 360° C sample stored in water (i.e. permanently hydrous) are so outstanding.

The electrodes calcined at $T > 360°$ C, Fig. 12a, show a completely different pattern. In particular, a large cathodic current precedes hydrogen evolution, and the charge spent in the range of $E < -0.65$ is recovered anodically in the same potential range while a pronounced anodic peak grows at about −0.4 V. Figure 12a also shows that the modifications occurring at $E < -0.65$ V are totally removed during the anodic sweep since the successive cathodic sweep is unaltered. This suggest that a (mild) cathodic treatment does not cause permanent surface alterations.

After recording the 'standard' voltammetric curve with the purpose of checking the surface charge, the samples were subjected to a more vigorous cathodic treatment. They were cycled from 0.35 V vs SCE to a potential where intense hydrogen evolution takes place, with a prolonged stop at the negative potential limit, each time increasing the dwell of the electrode at the potential. Thus, experiments were carried out with 10 s, 30 s, 1 min, 3 min, and 10 min dwells, after which the electrode was cycled within the 'standard' potential range for 3 min, and the 'standard' curve was finally recorded.

Figures 11b and 12b show the pattern not to change substantially with a stronger cathodic treatment. More specifically, the electrodes calcined at $T \leqslant 360°$ C, Fig. 11b, shows a very small current

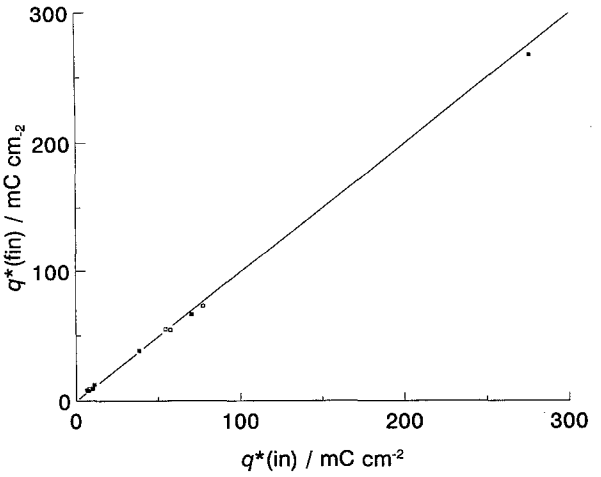

Fig. 13. Voltammetric charge at 20 mV s^{-1} measured after cathodic polarization experiments in 1 M NaOH solution (q_{fin}) (Part II of this study) against voltammetric charge measured before (q_{in}), for various IrO_2 electrodes stored in water (■) and in air (□). (——) Unit slope.

hysteresis thus indicating that the evolution of hydrogen is not accompanied by surface modificiations. Conversely, with electrodes calcined at $T > 360°$ C, Fig. 12b, two anodic peaks emerge after the cathodic discharge, although the surface is not permanently modified since the successive cathodic sweep is almost unaltered. Thus, if modifications take place, these involve the outer skin of the electrodes and can be removed during a single anodic scan. If the modifications penetrated the layer more deeply, an unbalanced anodic/cathodic charge ratio would persist in successive cycles in the 'standard' potential range.

That the surface of IrO_2 electrodes is not permanently modified by the cathodic treatment is confirmed by the data in Fig. 13 showing a plot of q^* from the 'standard' voltammetric curve immediately before and immediately after the whole cathodic treatment. Initial and final charges are linearly correlated: in particular they do not differ very much. Further, no systematic difference is observed depending on the conditions of storage. This behaviour is different from that observed with fresh samples, which exhibited a remarkable increase in q^* after the first cathodic treatment [12]. Such a different pattern is thought to indicate that the first cathodic treatment promotes the wetting of otherwise hydrophobic surface regions [12,13], the extension of the 'hydrophilic' surface being maintained thereafter, so that no more promotion of wetting is produced by futher hydrogen evolution. Figure 13 rather shows that, for the electrodes with the higher q^*, the charge value even tends to decrease slightly after hydrogen evolution, which presumably can be associated with some mechanical disruption (erosion) of the surface structure.

3.7. *Surface stability*

It has been mentioned in the experimental section that the 'standard' voltammetric curve recorded between

Table 1. Voltammetric charge of IrO_2 electrodes †

T/° C	*Medium*	*q**/mC cm^{-2}						
1	*2*	*3*	*4*	*5*	*6*	*7*	*8*	*9*
300	water	12	9.8	9.3	9.5	9.5	9.5	(‡)
	air	115	8.4	7.5	2.5	2.5	1.5	(‡)
330	water	116	93.5	77	64	62	58	(‡)
	air	127	91.5	73	66.5	66	48	(‡)
360	water	338	294	268	167	166	158	(‡)
	air	213	156	55	40	36	29.5	(‡)
400	water	42.5	38	38.5	43	53	49	40
	air	55	49	55	4.6	52	49.5	44
450	water	9.9	10.2	12	34	47	52	57
	air	7.6	8.2	9.1	31.5	37	39.5	45.5
500	water	6.7	6.7	8	21	26	30.5	39
	air	7.0	6.6	8	23.5	25	29	37.5

† Voltammetric curves recorded at 20 mV s^{-1} between −0.65 and 0.35 V vs SCE.
(1) Temperature of oxide calcination.
(2) Medium in which electrodes were stored between experiments.
(3) First determination ('fresh' electrodes for this study).
(4) During study of potential scan rate.
(5) After voltammetry into the hydrogen evolution region.
(6) After potential step experiments.
(7) After steady-state cathodic polarization curves.
(8) After measuring the order of reaction with respect to OH^-.
(9) After steady-state cathodic polarization curves at different temperatures.
(‡) The electrodes were visibly deteriorated with extensive loss of coating.

−0.65 and 0.35 V vs SCE constitutes a sort of 'fingerprint' of the electrode surface. Accordingly, the voltammetric charge can be used to monitor the conditions of the surface area. It has been shown elsewhere [26] that variations of q^* can reflect modifications in the morphology of the active layer.

Voltammetric charges were recorded after each set of experiments. A summary of the data is reported in Table 1. Electrodes prepared at $T \leqslant 360°$ C show a tendency for q^* to decrease, while for those calcined at $T > 360°$ C the trend of q^* is to increase. Apart from a more specific analysis, the general pattern indicates that the low-T layers, being poorly crystalline and therefore loosely bonded to the underlying metal, are progressively eroded during the various operations. It is interesting that just recording the voltammetric curves at various sweep rates produces a first dramatic decrease in q^*, especially for the samples with very high q^* values. It is also intriguing that mild hydrogen evolution does not cause major modifications, whereas a collapse in q^* is observed after repeated potential step experiments. It is plausible that proton penetration is induced more by potential steps than by hydrogen evolution so that the stability of the layer is undermined by any *sudden* swelling of particles and grain boundaries.

It is to be noted that while the samples prepared at 400° C do not show major changes, those at higher temperatures exhibit a sharp increase of q^* after the potential step experiments. It is not unreasonable to think that forced and prolonged proton penetration ultimately leads to 'open' the inner structure of the active layer otherwise made hydrophobic by 'dry' oxygen bridges. Thus, the increase in q^* reflects a factual increase in the working surface.

Finally, for layers calcined at $T \leqslant 360°$ C, the samples stored in the air seem more prone to erosion. This may be the result of 'dry' particles being less adherent

4. Conclusions

The electrochemical surface study carried out in this work proves that electrochemical techniques, although molecularly non-specific, can be very versatile giving simultaneous insight into a number of properties: chemical state, morphology, mechanical and electrochemical stability, extension of the active surface, solid state diffusion processes, etc. There are two major experimental parameters: (i) the 'standard' voltammetric curve monitoring the electrochemical surface spectrum, and (ii) the associated voltammetric charge, q^*, reflecting the morphology of the layer.

The temperature of 350° C appears to be a lower limit for obtaining IrO_2 by thermal decomposition of $IrCl_3$, although bulk experiments indicate [27] that the oxide is not formed below 500° C. Evidently, the presence of the support and the decomposition in a very thin layer make a difference. Below 350° C thermal decomposition is probably incomplete and the electrochemical response of the layer resembles the behaviour of the hydrous oxide anodically grown on metallic iridium [25] rather than that of a truly thermal oxide.

The different nature of the oxide layer causes also variable stability. The latter is higher for the high-T samples whereas those prepared at lower temperatures show a tendency to morphologically collapse.

Different conditions of storage (in water or in air) do not lead to major effects. It seems established that, once an oxide layer has achieved the maximum extension of the wetted surface with the first hydrogen evolution [28], this is retained unaltered for the rest of the electrode life irrespective of the conditions of storage.

Cathodic load does not cause appreciable effects on the state of the active layer. The present study cannot serve to exclude long-term effects, but it does show that these electrodes tend to be stable. In other words, the process of oxide reduction is located at the surface and its penetration (in any) is probably extremely slow. However, no tests of reductive chemical dissolution (if any) have thus far been carried out.

A study of the kinetics of hydrogen evolution will be reported in Part II of this work.

Acknowledgements

H.C. thanks TWAS (Trieste) for a fellowship. S.T. acknowledges the financial support of the CNR (Rome).

References

[1] H. B. Beer, *J. Electrochem. Soc.* **127** (1980) 303C.
[2] J. Horacek and S. Puschaver, *Chem. Eng. Prog.* **67** (1971) 71.
[3] D. M. Novak, B. V. Tilak and B. E. Conway, in 'Modern Aspects of Electrochemistry', Vol. 14 (edited by J. O'M. Bockris, B. E. Conway and R. E. White), Plenum, New York (1982) p. 195.
[4] E. Nicolas, *Eur. Pat. Appl. EP 23368* (1981); *Chem. Abstr.* **94** (1981) 199838.
[5] J. Clerc-Renaud, F. Leroux and D. Ravier, *Eur. Pat. Appl. EP 240413* (1987); *Chem. Abstr.* **108** 45864.
[6] J. F. Cairns, D. A. Denton and P. A. Izard, *Eur. Pat. Appl. EP 129374* (1984); *Chem. Abstr.* **102** (1985) 102442.
[7] A. Nidola, PCT *Int. Appl. WO 86 03790* (1986); *Chem. Abstr.* **105** (1986) 122974.
[8] E. R. Kötz and S. Stucki, *J. Appl. Electrochem.* **17** (1987) 1190.
[9] M. Jaccaud, F. Leroux and J. C. Millet, *Mater. Chem. Phys.* **22** (1989) 105.
[10] A. Anani, Z. Mao, S. Srinivasan and A. J. Appleby, *J. Appl. Electrochem.* **21** (1991) 683.
[11] D. Galizzioli, F. Tantardini and S. Trasatti, *ibid.* **5** (1975) 255.
[12] J. F. C. Boodts and S. Trasatti, *ibid.* **19** (1989) 255.
[13] J. F. C. Boodts, G. Fregonara and S. Trasatti, in 'Performance of Electrodes for Industrial Electrochemical Processes' (edited by F. Hine, B. V. Tilak, J. M. Fenton and J. D. Lisius), The Electrochemical Society, Pennington, NJ (1989) p. 135.
[14] S. Trasatti, in 'Modern Chlor-Alkali Technology', Vol. 5 (edited by T. C. Wellington), Elsevier, Amsterdam (1992) p. 281.
[15] S. Ardizzone, A. Carugati and S. Trasatti, *J. Electroanal. Chem.* **126** (1981) 287.
[16] R. Garavaglia, C. M. Mari and S. Trasatti, *Surf. Technol.* **23** (1984) 41.
[17] S. Trasatti, *Electrochim. Acta* **36** (1991) 225.
[18] G. Lodi, E. Sivieri, A. De Battisti and S. Trasatti, *J. Appl. Electrochem.* **8** (1978) 135.
[19] S. Ardizzone, D. Lettieri and S. Trasatti, *J. Electroanal. Chem.* **146** (1983) 431.
[20] A. J. Bard, J. Jordan and R. Parsons (Eds), 'Standard Potentials in Aqueous Solution', Dekker, New York (1985).
[21] Yu. B. Makarychev, E. K. Spassakaya, S. D. Khodkevich and L. M. Yakimenko, *Elektrokhimiya* **12** (1976) 994.
[22] R. F. Savinell, R. L. Zeller and J. A. Adams, *J. Electrochem. Soc.* **137** (1990) 489.
[23] S. Ardizzone, G. Fregonara and S. Trasatti, *Electrochim. Acta* **35** (1990) 263.
[24] K. Doblhofer, M. Metikoš, Z. Ogumi and H. Gerischer, *Ber. Bunsenges. Phys. Chem.* **82** (1987) 1046.
[25] J. Mozota and B. E. Conway, *J. Electrochem. Soc.* **128** (1981) 2142.
[26] R. Boggio, A. Carugati, G. Lodi and S. Trasatti, *J. Appl. Electrochem.* **15** (1985) 335.
[27] G.-W. Jang and K. Rajehwar, *J. Electrochem. Soc.* **134** (1987) 1830.
[28] S. Ardizzone, G. Fregonara and S. Trasatti, *J. Electroanal. Chem.* **266** (1989) 191.